Hysteresis and multiple stable configurations in a magnetic fluid system

# Hysteresis and multiple stable configurations in a magnetic fluid system

## D P Jackson

Department of Physics and Astronomy, Dickinson College, Carlisle, PA 17013, USA

E-mail: jacksond@dickinson.edu

## Abstract

A magnetic liquid in a horizontal Hele–Shaw cell is subjected to a vertical magnetic field. The width of the magnetic fluid finger is measured as a function of applied field and compared to a theoretical model. The theoretical model uses an energy minimization procedure and predicts a double energy minimum, hysteresis, and discontinuous transitions between a circle and a finger. The experimental data set agrees very well with the theory for a well-defined magnetic fluid finger. Near the transitions, the experiments show hysteresis and support for a double energy minimum; however, the agreement is not quite so good. The discrepancy between theory and experiment near the transition region is likely due to the simplified finger model used in the theory.

(Some figures in this article are in colour only in the electronic version)

## 1. Introduction

When a magnetic fluid is trapped with an immiscible fluid between two closely-spaced horizontal plates and subjected to a vertical magnetic field, a fingering instability results in the magnetic fluid evolving into a complex, branched pattern [1, 2]. Depending on various parameters of the applied magnetic field [3], the final state pattern can be a relatively simple short 'finger' in the shape of a 'dumbbell', or a highly convoluted maze-like labyrinthine structure (see figure 1). In addition, several investigations of multiple magnetic fluid drops have demonstrated some degree of predictability in the final state patterns [4–7].

In all of the patterns shown in figure 1, the magnetic liquid has a fairly well-defined finger width. In the labyrinthine pattern, the spacing between fingers is also quite well defined. Although the finger width and spacing in these labyrinthine patterns was initially investigated over twenty years ago [8], some recent work has corrected and expanded on the previous results and explored three different methods for computing the magnetic energy of this system [9, 10]. In [10], it is shown that the assumption of a constant demagnetizing field (called method B) leads to results that agree with experiments only for small applied fields, while two other methods (called A and C) are effectively indistinguishable and agree with experiments for all applied field values.

Until recently, all theoretical and experimental investigations into the width of a magnetic fluid finger have centered on labyrinthine patterns. This is a bit surprising because the calculations involve an infinite number of infinitely long fingers and are therefore difficult to carry out. For similar reasons, experiments are easily plagued in some way by 'edge' effects, e.g. nonuniformities in the applied field or the boundaries of the Hele–Shaw cell. In contrast, both theoretical and experimental investigations are simplified a great deal by considering a system composed of a single magnetic fluid finger (leftmost image in figure 1).

In this paper, we expand on our previous investigation of a single magnetic fluid finger in a horizontal Hele–Shaw cell subjected to a vertical magnetic field [11]. First, we present the theoretical model used to calculate the finger width and discuss some surprising features of this model. Second, we present some experimental results for this system and compare these results to the theoretical predictions. Finally, we conclude with a discussion of the results and some suggestions for future work.

## 2. Theory

In general, the total energy of a magnetic fluid system consists of three pieces: gravitational, surface, and magnetic. For a magnetic fluid in a horizontal Hele–Shaw cell, the gravitational
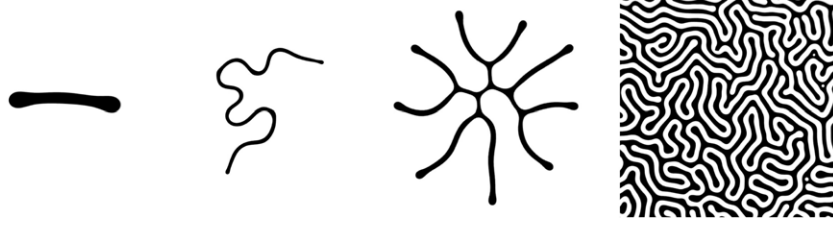
**Figure 1.** Some typical magnetic fluid patterns, from a simple finger (left) to a complex labyrinth (right). The simple finger is investigated in this paper.
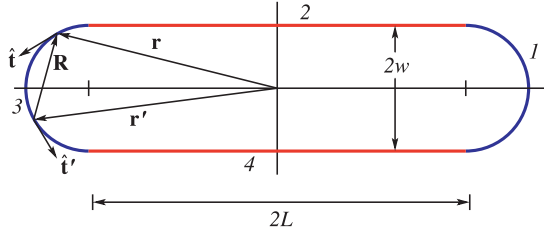


**Figure 2.** A model of an idealized ferrofluid finger consisting of two parallel line segments of length $2L$ and two semicircles of radius $w$.

energy is constant and can be neglected. This leaves only the surface and magnetic energies. The surface energy is given by

$$E_{\mathrm{s}} = \sigma h P, \qquad (1)$$

where $\sigma$ is the surface tension, $h$ is the plate spacing in the Hele–Shaw cell, and $P$ is the perimeter of the domain. In order to determine the field energy, we assume that the magnetization of the magnetic fluid in a uniform magnetic field is both uniform and constant, an assumption first introduced by Cebers and Maiorov [12]. This corresponds to method C in [10]. Note that although the magnetization is assumed to be uniform, the demagnetizing field is not. It is precisely this 'fringing field' that gives rise to the fingering instability in this model [13]. Using this model, the magnetic energy for an arbitrarily-shaped domain is given by [14]

$$E_{\mathrm{m}} = \frac{\mu_0 h M^2}{2}\left[A - \frac{1}{2\pi}\oint \mathrm{d}s \oint \mathrm{d}s'\,\hat{\mathbf{t}}\cdot\hat{\mathbf{t}}'\,\Phi(R/h)\right], \quad (2)$$

where $\mu_0$ is the permeability of free space, $M$ is the magnetization of the ferrofluid, and $A$ is the area of the domain as seen from above. The integration is carried out over the perimeter of the domain with $s$ and $s'$ representing arc-length coordinates along the contour of the domain, and $\hat{\mathbf{t}}$ and $\hat{\mathbf{t}}'$ are unit tangent vectors at $s$ and $s'$, respectively (figure 2). The distance between $s$ and $s'$ is given by $R = |\mathbf{r} - \mathbf{r}'|$ and $\Phi(\xi) = \sinh^{-1}(1/\xi) - \sqrt{1+\xi^2} + \xi$ is a coupling strength that arises from integration over the height of the domain.

In order to calculate the energy of a single finger, the shape of the magnetic fluid domain must be specified. As seen in the leftmost image of figure 1, the precise shape of a magnetic fluid finger has slightly bulbous tips and would be very difficult to specify exactly. An idealized model is used that assumes the finger is perfectly straight, constant in

width, and has ends consisting of semicircles (see figure 2). The perimeter of the domain is partitioned into four segments: two straight lines of length $2L$ and two semicircles of radius $w$ (note that $L$ and $w$ are not independent). These segments are numbered 1–4 beginning with the right semicircle and moving counterclockwise around the domain.

Using this parametrization in equation (2) leads to 16 separate double integrals, one for each pair of segments. Fortunately, symmetry immediately reduces the number of independent integrals to five. This allows us to write down the total energy for a magnetic fluid finger in dimensionless form as (see [11] for details)

$$\tilde{E} = E/\sigma R_0{}^2 = \frac{2\pi}{p}\left(\frac{1+\tilde{w}^2}{\tilde{w}}\right)$$
$$+ N_{\mathrm{B}}\pi^2\left(1 - \frac{1}{\pi^2}\sum_{i=1}^{5}J_i(\tilde{w})\right), \qquad (3)$$

where $\tilde{w} = w/R_0$ is the scaled finger width, $p = 2R_0/h$ is the aspect ratio, $N_{\mathrm{B}} = \mu_0 M^2 h/(2\pi\sigma)$ is the (dimensionless) magnetic bond number, and the $J_i$ are dimensionless integrals defined in the appendix of [11].

For a fixed plate spacing and magnetic field value, equation (3) gives the total energy of a magnetic fluid finger in an applied field in terms of the single parameter $\tilde{w}$. This parameter $\tilde{w} = w/R_0 = 2w/2R_0$ is simply the width of the finger scaled by the initial diameter of the circle. Thus, a value of $\tilde{w} = 1$ corresponds to a circle and as $\tilde{w}$ decreases, the finger becomes longer and thinner. The energy of a circular ferrofluid domain can be written in terms of complete elliptic integrals [12, 14] and should be identical to equation (3) with $\tilde{w} = 1$. Numerical calculations demonstrate that this is indeed the case.

Figure 3 demonstrates the behavior of the finger energy given by equation (3). The left graph shows the total energy as a function of finger width for a fixed aspect ratio $p = 7.2$, and three magnetic bond numbers, $N_{\mathrm{B}} = 1.0$, 1.5, and 1.8. For convenience, the energies are scaled by the energy of a circular domain with the same magnetic field value. The location of each minimum corresponds to the preferred finger width. For low magnetic fields (low $N_{\mathrm{B}}$), the energy is minimized when $\tilde{w} = 1$ (a circle). As the magnetic field increases, the minimum shifts toward $\tilde{w} = 0$ demonstrating that the preferred finger width decreases.

Interestingly, near the transition from a circular domain to a finger, the energy has a double-well behavior. That is, the model predicts two stable configurations for a range of applied
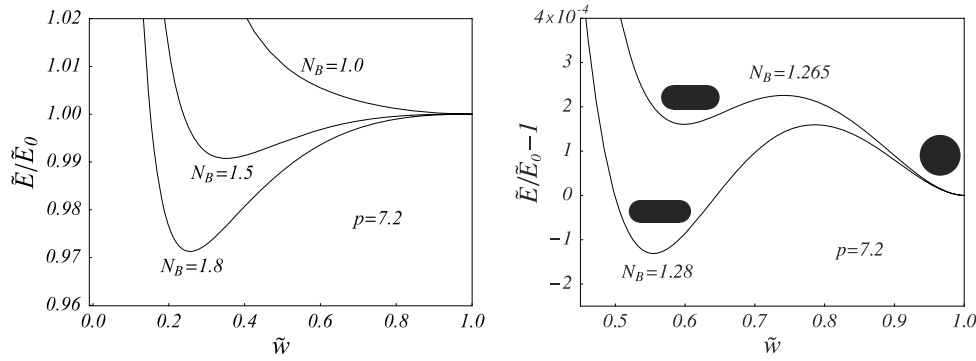
**Figure 3.** Left: energy as a function of finger width for a fixed aspect ratio, $p = 7.2$, and three different magnetic bond numbers. The energies are calculated using equation (3) and scaled by the energy of a circular domain. Right: for a particular range of bond numbers, the energy has two distinct minima, giving rise to two configurations as shown.

field values. This is demonstrated on the right graph in figure 3. Here, the energy is plotted using $p = 7.2$ for $N_B = 1.265$ and $N_B = 1.28$. Note the change in scale to emphasize this double minimum.

One immediate consequence of this behavior is that the preferred finger width first appears with a finite value. That is, the system is predicted to undergo a first-order transition as it abruptly changes from a circle to a finite finger. This happens because there is a barrier that separates the two energy minima. Therefore, as the magnetic field is increased, the system will stay trapped in the circular state ($\tilde{w} = 1$) until the barrier disappears. Conversely, once a finger has formed and the magnetic field is decreased, the system will now stay trapped in the finger state ($\tilde{w} < 1$) until the barrier disappears. Since these two transitions occur for different magnetic field values, the system exhibits a subcritical pitchfork bifurcation with the associated hysteresis that is common in such systems. This agrees with the numerical results obtained by Cebers and Zemitis [15].

## 3. Experiment

Figure 4 shows a schematic of the experimental setup. A Hele–Shaw cell consisting of two 30 cm × 30 cm × 0.6 cm glass plates separated by a 1 mm spacer is placed at the center of a Helmholtz coil arrangement capable of producing magnetic fields up to 0.034 T. The Hele–Shaw cell is backlit and images are obtained using a CCD camera. The entire system is computer controlled [16] and the resulting high contrast images are relatively simple to analyze.

The experimental procedure is reasonably straightforward. The applied magnetic field is increased in small steps and the magnetic liquid is imaged after it has come to rest. Unfortunately, the magnetic liquid tends to stick to the glass plates which makes it very difficult to obtain reproducible data. To try to eliminate this problem, the glass plates are thoroughly cleaned before constructing the Hele–Shaw cell. Next, a solution of Tween-80 (polyoxyethylenesorbitan monooleate) and distilled water is inserted into the cell. After letting it sit for a few days, the cell is flushed with distilled water and the process is repeated. Just prior to running an experiment,
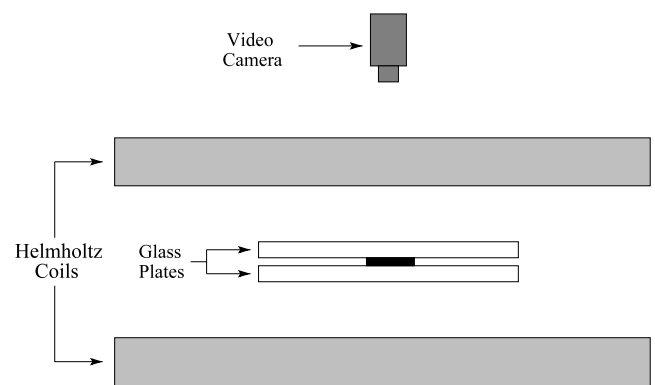


**Figure 4.** Schematic diagram of the experimental setup. The Hele–Shaw cell with the magnetic fluid is placed inside a pair of Helmholtz coils. The magnetic fluid evolution is captured with a CCD camera.

the cell is filled with either pure water or the water/Tween mixture and then the immiscible magnetic liquid is injected. Unfortunately, even this rather laborious procedure does not always lead to stick-free results. Typically, one portion of the cell will remain relatively clean and stick free for at least a few hours, providing a reasonable opportunity to perform the experiment.

For the experiments presented here, a mineral-oil based ferrofluid (EFH1) manufactured by FerroTec Corporation is used[1]. This ferrofluid has an initial susceptibility of $\chi_i = 1.70$ and a saturation magnetization of $\mu_0 M_s = 0.040$ T.

In the first experiment (previously reported in [11]), the cell is prepared using a 0.25% water/Tween solution and this same solution is used as the immiscible liquid in the Hele–Shaw cell. As the magnetic field is increased, the magnetic liquid is gently prodded with a small hand magnet to see if it relaxes back to a circle or grows into a finite finger. When the magnetic liquid appears to stop moving, a picture is taken before proceeding with another measurement. Because the ferrofluid has a tendency to stick to the glass plates, multiple measurements are made at each magnetic field value. In

---

[1] EFH1 ferrofluid is widely available through a number of educational suppliers. See [17] for more information.
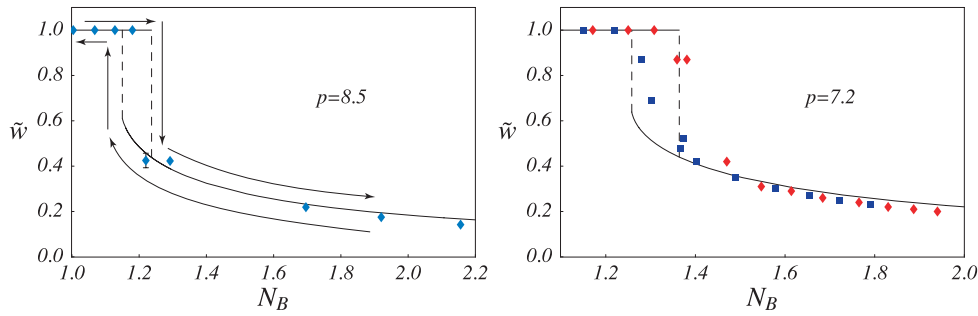
**Figure 5.** Left: a comparison of experimental results and the theoretical prediction for $p = 8.5$. The data points represent averages of 'growing' (field ramped up) and 'shrinking' (field ramped down) measurements. The arrows denote the predicted path of the magnetic liquid and demonstrates the hysteresis in this system. Right: a more recent experiment for $p = 7.2$. Diamonds (red) represent 'growing' measurements and boxes (blue) represent 'shrinking' measurements.



| 201 G | 204 G | 202 G | 203 G |
| (ramped up) | (ramped up) | (ramped down) | (ramped down) |

**Figure 6.** Equilibrium patterns of a magnetic liquid in a Hele–Shaw cell for (approximately) the same magnetic field values differ depending on whether the field is ramped up or down. The patterns are (nearly) circular when the field is ramped up and elongated when the field is ramped down. This clearly demonstrates hysteresis and a double energy minimum. The final magnetic field values correspond to bond numbers between 1.36 and 1.38.

each case, the final field is approached from below and from above so the ferrofluid is growing in one case and shrinking in the other. Thus, if sticking is a problem, a growing finger is expected to be slightly shorter and fatter than a shrinking finger. We found very little difference between the growing and shrinking fingers indicating that sticking was not a major problem in this experiment.

The left graph in figure 5 shows the experimental data and the theoretical prediction for this experiment. Each data point is an average of four separate measurements, two in which the magnetic field was approached from below (growing finger) and two in which the field was approached from above (shrinking finger). The arrows in the graph denote the predicted path of the magnetic liquid as the field is increased and then decreased.

To compare experiment to theory, the magnetic liquid is assumed to obey a superparamagnetic magnetization law as given by the Langevin equation $M = M_s(\coth \alpha - 1/\alpha)$, where $\alpha = 3\chi_i B/(\mu_0 M_s)$ [18]. It is also necessary to know the surface tension of the magnetic liquid in our Hele–Shaw cell. This is determined by looking for the magnetic field when the droplet first becomes unstable and comparing this to the critical bond number for elliptic instability [12]. For this experiment, the surface tension is found to be $\sigma = 0.030$ N m$^{-1}$. Finally, since the experimental fingers do not have a perfectly uniform width, it is not completely clear how to determine the finger width from the raw data. We calculate the scaled finger width from the so-called Heywood Circularity Factor, which gives the ratio of the perimeter of a finger to the circumference of a circle with the same area. More detail on these procedures can be found in [11].

As can be seen in the left graph in figure 5, the data shows very good agreement with the theoretical predictions, even near the transition points. Unfortunately, this experiment did not show evidence of two stable configurations. A more recent experiment was performed using the same magnetic liquid (EFH1). In this experiment, the Hele–Shaw cell was prepared using a 2% solution of water and Tween-80 and the experiment was performed using pure (distilled) water as the immiscible liquid. This led to a surface tension of $\sigma = 0.057$ N m$^{-1}$, surprisingly different from the previous experiment.

In this second experiment, sticking appeared to be much less of a problem. The magnetic field was simply ramped up or down and an image was taken when the magnetic liquid stopped moving. The results of this experiment are shown in the right graph of figure 5. Again, the overall agreement with the theoretical prediction is quite good, except near the transition region. This is discussed in more detail in the next section. The (red) diamonds represent data when the field is ramped up to a higher value and the (blue) boxes represent data when the field is ramped down to a lower value. Hysteresis is evident in this data; the circle-to-finger transition occurs at a higher bond number than the finger-to-circle transition.

In fact, we observe very clearly and reproducibly that ramping up to a particular magnetic field value leads to a different shape than ramping down to (approximately) the same field value. Figure 6 demonstrates this behavior. The two images on the left show the final pattern when the field is ramped from zero up to final field values of 201 and 204 G.[2]

[2] The final field values are not exactly the same due to temperature changes in the Helmholtz coils. We control the voltage from the power supply but the resistance of the coils changes throughout the experiment.

The patterns begin as circles and at first glance, they appear to remain circular, however, a closer inspection reveals they are not. A circle has been drawn around the images to demonstrate this. The right two images show the final patterns when the field is ramped down to 202 and 203 G. This supports the idea that the system really has two energy minima and can be directed into either minimum through careful manipulation of the applied field (see figure 3).

## 4. Discussion and conclusions

Let us now return to examine the data in figure 5 in more detail. The latest data shown in the right graph demonstrates a couple of interesting features. First, beyond the transition region—when the bond number is greater than about 1.5— the data is quite smooth and in very good agreement with the theoretical prediction regardless of whether the field is ramped up or down. This suggests that the simple model shown in figure 2 is a good approximation for an actual magnetic fluid finger. Second, the experimental data appears to demonstrate hysteresis in the system, an indication that there are indeed multiple minima in the energy. However, the transition region does not agree quite so well with the theoretical predictions and the transitions appear to be smoother than the discontinuous nature of the model. It is much more difficult to obtain experimental data in this region because the shape of the magnetic liquid depends very sensitively on the applied field. Thus, while it is clear from the data that the circle does *not* jump discontinuously from a circle to a finite finger, it is still not clear whether the transition is completely smooth or whether there is a discontinuous jump somewhere in the transition region.

The most obvious reason for the discrepancy between the theory and experiment is because the finger model is simply not terribly accurate in the transition region. A comparison of the experimental and theoretical finger shapes (see figure 6 and the right graph in figure 3) shows that this is not particularly surprising. To accurately capture the hysteresis region theoretically will require a more realistic model for the magnetic fluid finger. One possible model is the so-called ovals of Cassini, a model used to study shape transitions in lipid monolayers [19]. These researchers employed a strictly two-dimensional analysis and demonstrate qualitatively similar results to what we observe here. Employing such a model for a three-dimensional magnetic liquid system should result in a more accurate description of the transition region.

## References

[1] Rosensweig R E 1985 *Ferrohydrodynamics* (Cambridge: Cambridge University Press) pp 208–16
[2] Blums E, Cebers A O and Mairov M M 1997 *Magnetic Fluids* (Berlin: Walter de Gruyter) pp 206–40
[3] Dickstein A J, Erramilli S, Goldstein R E, Jackson D P and Langer S A 1993 *Science* **261** 1012–5
[4] Drikis I, Bacri J-C and Cebers A O 1999 *Magnetohydrodynamics* **35** 157–69
[5] Jackson D P and Gantner B 2001 *Phys. Rev.* E **64** 056230
[6] Jackson D P 2003 *Phys. Rev.* E **68** 035301(R)
[7] Jackson D P 2005 *J. Magn. Magn. Mater.* **289** 188–91
[8] Rosensweig R E, Zahn M and Shumovich R 1983 *J. Magn. Magn. Mater.* **39** 127–32
[9] Richardi J, Ingert D and Pileni M P 2002 *J. Phys. Chem.* B **106** 1521–3
[10] Richardi J, Ingert D and Pileni M P 2002 *Phys. Rev.* E **66** 046306
[11] Hillier N J and Jackson D P 2007 *Phys. Rev.* E **75** 036314
[12] Cebers A O and Maiorov M M 1980 *Magnetohydrodynamics* **16** 21–7
[13] Jackson D P, Goldstein R E and Cebers A O 1994 *Phys. Rev.* E **50** 298–307
[14] Langer S A, Goldstein R E and Jackson D P 1992 *Phys. Rev.* A **46** 4894–904
[15] Cebers A O and Zemitis A A 1983 *Magnetohydrodynamics* **19** 360–8
[16] We use LabVIEW, available from National Instruments, Inc. www.ni.com
[17] www.ferrotec.com
[18] Rosensweig R E 1985 *Ferrohydrodynamics* (Cambridge: Cambridge University Press) pp 55–61
[19] de Koker R and McConnell H M 1993 *J. Phys. Chem.* **97** 13419–24